JACS
JOURNAL OF THE AMERICAN CHEMICAL SOCIETY
Article
pubs.acs.org/JACS

Li-Filled, B-Substituted Carbon Clathrates

Tao Zeng,[†,‡] Roald Hoffmann,[*,†] Reinhard Nesper,[§] N. W. Ashcroft,[∥] Timothy A. Strobel,[⊥] and Davide M. Proserpio[#,▽]

[†]Baker Laboratory, Department of Chemistry and Chemical Biology, Cornell University, Ithaca, New York 14853, United States
[‡]Department of Chemistry, Carleton University, Ottawa, Ontario K1S5B6, Canada
[§]Laboratory of Inorganic Chemistry, ETH Zürich, Vladimir-Prelog-Weg 1, CH-8093 Zürich, Switzerland
[∥]Laboratory of Atomic and Solid Physics, Cornell University, Ithaca, New York 14853, United States
[⊥]Geophysical Laboratory, Carnegie Institution of Washington, 5251 Broad Branch Road NW, Washington, D.C. 20015, United States
[#]Dipartimento di Chimica, Università degli Studi di Milano, 20133 Milano, Italy
[▽]Samara Center for Theoretical Materials Science (SCTMS), Samara State University, Samara 443011 Russia

Supporting Information

ABSTRACT: Inside the cages of hypothetical carbon clathrates there is precious little room, even for the smallest atoms, such as Li—unless it is the Li^+ ion that is inserted, in which case a compensating negative charge should be distributed over the carbon cage. The hypothesis explored in this paper is that Li insertion can be achieved with appropriate B substitution within the framework. The resulting structures of $2Li@C_{10}B_2$ (Clathrate VII), $8Li@C_{38}B_8$ (Clathrate I), $7Li@C_{33}B_7$ (Clathrate IV), $6Li@C_{28}B_6$ (Clathrate H), and $6Li@C_{28}B_6$ (Clathrate II) are definitely stabilized in theoretical calculations, especially under elevated pressure, as judged by enthalpy criteria and bond length metrics. Different strategies for B substitution (symmetry reduction, following the parent charge distribution, and substitution on the most weakened bonds, relieving stress on bond angles) are explored. Two possible competing channels for Li doping−B substitution, formation of LiBC and C-vacancies, are investigated.

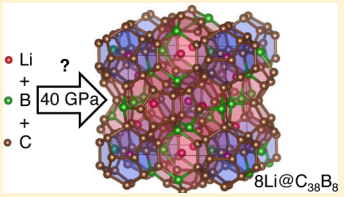

INTRODUCTION

What are commonly called clathrate structures self-assemble everywhere in chemistry where space is filled with approximately tetrahedral building blocks, and where fewer or greater than four contacts are electronically discouraged. Among the common structural constituents of clathrate structures—let's call them nodes—are water molecules, Group 14 elements, or SiO_2.[1−12]

An infinity of low-energy structural minima of high density for such four-coordinated nodes is obtained in the stacking variants of the diamond structure, or from interpenetrating diamondoid nets, if the node−node separation is large. The characteristic features of clathrates are (a) polyhedral structures, built mostly of 4- to 6-membered rings with cavities substantially bigger than those of the diamondoid networks, and (b) angles and distances not that different from the optimum tetrahedral angle and node−node separation of the diamond archetype. The net result of these features, essentially constraints of Euclidean space coupled with bond metrics, is that the clathrate structures are (c) less dense than diamonds, yet (d) per node, not that much less stable than the global energy minimum of the diamond family. A further consequence—let's call it a lure—is that the cavities of the polyhedra of carbon clathrates seem to be waiting there to be filled with other atoms, as they are in other Group 14 clathrates.

Our paper sets out the exploration of some as yet unsynthesized carbon clathrates, substituted by B atoms and stuffed with Li atoms.

Clathrates and the Special Problems of Those Made of Carbon. In Figure 1 we show five typical clathrate structures; for a more complete list, please see the Reticular Chemistry Structural Resource[13,14] or the database of zeolite structures.[15] The building blocks of these clathrates are a variety of polyhedra with typical ideal bond angles within 20 degrees of the tetrahedral angle; the $[5^{12}]$ and $[5^{12}6^2]$ polyhedra are most common, clearly seen in the structure of Clathrate I.[16,17] An exceptionally clear and useful survey of Group 14 clathrate structures has been given by Karttunen, Fässler, and co-workers;[18] we will have occasions to refer to this paper repeatedly. Historically, many studies have looked at the stability of C clathrates at P = 1 atm and under compression; one of us (RN) has contributed an early example.[19−37] No carbon clathrates have been made, to our knowledge. But we mention here the products of fullerene pressurization obtained and characterized by the Yamanaka group—C_{60} buckyballs that are connected in three dimensions through 4-coordinated carbons.[38−41]

In Table 1, we list some calculated properties of the clathrates investigated in this paper. They compare well with

Received: July 27, 2015
Published: September 14, 2015

DOI: 10.1021/jacs.5b07883
J. Am. Chem. Soc. 2015, 137, 12639−12652

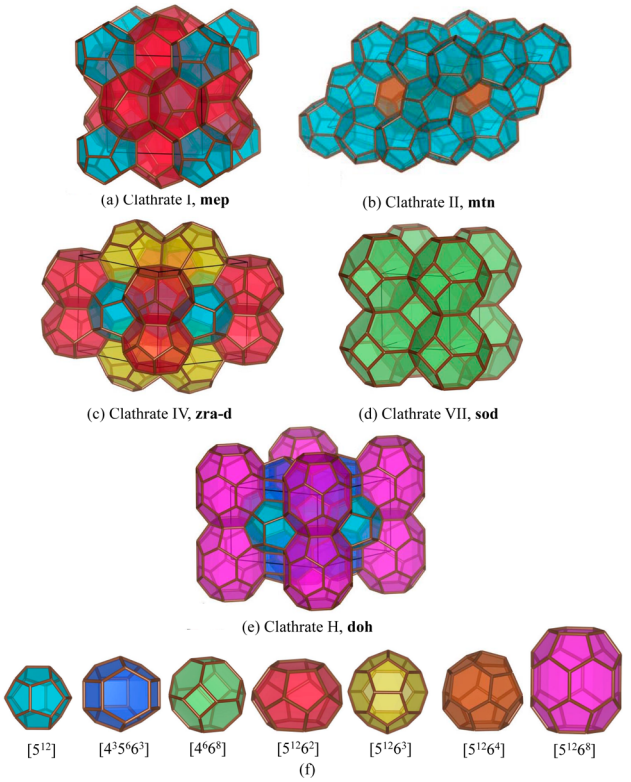

Figure 1. (a)−(e) Structures of the five clathrates investigated in this work. (f) The building blocks of the structures.

those presented in ref 18 (except band gaps, more details below), although different basis sets (plane wave here and atomic functions there) and functionals are used.

The optimized geometries are from our calculations (details in Computational Methods section at the end of paper)—all calculations are done with the pressure 1 atm unless further specified. And all are static ground state calculations, without addition of zero point energies. All unit cell coordinates of the calculated structures in this work are given in the TXT file in the Supporting Information (SI).

Let's take Clathrate I as an example — in its optimized structure, we get a range of CC distances between 1.52 and 1.59 Å, and a range of CCC bond angles between 106 and 124°. The resultant density (3.05 g/cm^3) is intermediate between graphite and diamond. The net result of the small geometrical deformations noted is an enthalpy only 0.11 eV/C relative to diamond for C Clathrate I.

Yet no carbon clathrate framework has been made, as we said. When it is made, carbon Clathrate I will most certainly be kinetically persistent—it takes much energy to disrupt CC bonds on the way to diamond. Considering that buckminsterfullerene is about 0.39 eV/C less stable than diamond but is very much bench-stable, we believe all five carbon clathrates in Table 1 are likely to have substantial kinetic stability.

The cavities in these clathrates are enticing. For other Group 14 elements, Si, Ge, and Sn, quite persistent, colloquially "stable" compounds exist in which these cavities are filled with a variety of atoms, yielding stoichiometries such as Na_8Si_{46}, K_8Si_{46}, and Ba_8Si_{46}.[42−46] But for carbon, there is just less room in the cavities to encapsulate a guest atom. How much less, we will examine in detail below. It might also be noted that in alkali-metal-doped Group 14 clathrates, the metal atoms do not necessarily go into the cavities. So there was a recent report that in $K_8Li_xGe_{44-x/4}\square_{2-3x/4}$ ($\square$ being vacancies on the cage) Clathrate I structure, the Li atoms occupy cage sites,[47] i.e., when all cavities are occupied by K, Li are "marginalized" to the cage. This type of ternary compound is not considered in the present study.

The difficulty of stuffing atoms in the carbon clathrates can be seen in another, very direct, way from calculating the enthalpy of inserting 8 Li atoms into Clathrate I, which has 8 polyhedra per 46 atoms unit cell. This turns out in our calculations to be[48]

Table 1. Calculated Properties of the Five Carbon Clathrates Investigated in This Paper

structure[a]	polyhedral components[b]	relative enthalpy[c] (eV/atom)	r_{CC} range (Å)	∠CCC range (°)	"radii" of polyhedra[d]	band gap[e] (eV)	Li-doping enthalpy (eV/Li)
I (C_{46}, **mep**)	$[5^{12}]_2[5^{12}6^2]_6$	0.11	1.52−1.59	106−124	2.17, 2.41 2.14, 2.27	3.9, 5.6	2.31
II (C_{34}, **mtn**)[f]	$[5^{12}]_4[5^{12}6^4]_2$	0.08	1.53−1.59	106−120	2.17, 2.61 2.09, 2.58	3.7, 5.5	2.28
IV (C_{40}, **zra-d**)	$[5^{12}]_3[5^{12}6^2]_2[5^{12}6^3]_2$	0.13	1.51−1.66	105−124	2.16, 2.43, 2.53 2.08, 2.28, 2.47	3.5, 5.1	2.20
VII (C_{12}, **sod**)	$[4^66^8]_2$	0.39	1.55	90−120	2.45 2.45	2.6, 3.6	2.66
H (C_{34}, **doh**)	$[5^{12}]_3[4^35^66^3]_2[5^{12}6^8]_1$	0.14	1.53−1.57	90−120	2.18, 2.20, 2.97 2.13, 2.03, 2.77	2.7, 4.3	2.30

[a]Given in the parentheses are the unit cell formula and the RCSR three-letter name (http://rcsr.anu.edu.au/) of the clathrate. [b]The subscript digit indicates the number of the bracketed polyhedra in the unit cell. [c]Relative to diamond, calculated with our approximations. [d]Averaged (shortest) distances between the center of mass of a polyhedron and its vertices are given in the upper (lower) row. The values are ordered in the same sequence as the types of polyhedra in the second column. The two sets of data largely follow the same order. [e]The two values correspond to the gap extracted from the conventionally calculated DOS and the G0W0 gap. [f]Throughout this paper, we use the primitive cell, 34 C atoms, in the study of Clathrate II and its relevant Li-doped and B-substituted structures, instead of the conventional cell with 136 C atoms.

DOI: 10.1021/jacs.5b07883
J. Am. Chem. Soc. 2015, 137, 12639−12652

$$8\text{Li(bcc)} + \text{C}_{46}(\text{Clathrate I}) = 8\text{Li@C}_{46}$$
$$\Delta H = 2.31 \text{ eV/Li} \quad (1)$$

We will return to the electronic reason for this destabilization, and its structural consequences.

No reason to give up. Let's think about inserting into the clathrate cavities an ion, for ionic radii are much smaller than covalent or van der Waals ones. The obvious candidates are Li^+ and Be^{2+}. Electrostatically, it is obvious that one must make the clathrate cage anionic, when cations are inserted. This may be accomplished by substituting isoelectronic B^- for C, so that the Li-doped, B-substituted structure is isoelectronic to its parent C clathrate, and (we argue) inherits its stability. For Clathrate I, the extended structure we want has the stoichiometry $Li_8B_8C_{38}$. Actually, similar Group 1 element-doped and Group 13 element-substituted clathrates of Group 14 elements other than C have been synthesized and investigated, e.g., $K_8Ga_8Si_{38}$, $Rb_8Ga_8Si_{38}$, and $K_7B_7Si_{39}$,[49−51] as well as some Group 2 element-doped clathrates.[52−55] But we need to re-emphasize the trouble on our hands: C is not Si, and the cavities in the carbon clathrates are small! The cavity radii of the carbon polyhedra are smaller than those of the silicon counterparts by at least 1 Å (see Table 3 of ref 18).

In our thinking about compensating the positive charge on the inserted Li^+ ions with the negative charge on B^- substituting for C, we avoid other Group 13 elements, such as Al (which are fine in Si and Ge clathrates[56,57]). This is because the size of B is comparable to C,[58] and there might be little structural penalty in strain to the clathrate framework. But exactly how comparable are B^- and C? One measure may be obtained from a Cambridge Structural Database[59] search on borate anions. This, of course, found many tetraphenyl borates, but also a few other compounds, with a range of B−C distances of 1.62−1.67 Å.[60−62] We also obtained a theoretical measure, by optimizing the structure of $B(CH_3)_4^-$ (section S2 in the SI), isoelectronic with neopentane. The B−C distance in this anion comes out as 1.65 Å, compared with the 1.54 Å C−C distance in neopentane. It looks like a B^- center is about 0.1 Å larger than a C.

There are other phases in the Li/B/C ternary phase diagram. One of these, LiBC, will be considered by us as a thermodynamic competitor phase. $Li_2B_{12}C_2$ (as well as $Li_2B_{12}Si_2$ and $Li_2B_{12}PC$) exist,[63−65] featuring typical icosahedral B_{12} cages. We will not consider these fascinating, but topologically distinct phases. We mention finally another strategy to implant alkali metal ions into C cages, put into practice for fullerenes. This is to exploit counter-anions, e.g., $[Li^+@C_{60}]$ $[SbCl_6^-]$[66] and $[Li^+@C_{60}]$ $[PF_6^-]$.[67] However, this strategy is only applicable when each cage is an isolated molecular entity.

With the stage set, we now explore the geometries and energetics of the formation of a variety of Li-encapsulated, B-substituted carbon clathrates.

RESULTS AND DISCUSSION

Clathrate VII: A Less Stable Clathrate with a Small Unit Cell. We start our journey with one of the smallest and simplest (in terms of the number of types of polyhedra and the number of C atoms in a unit cell) clathrates, Clathrate VII.[68] It contains only one type of polyhedron, $[4^6 6^8]$, and all C atoms are identical by symmetry. SiO_2 with the similar polyhedron building unit is called sodalite. Although it is the least stable (0.39 eV/C atom relative enthalpy with respect to diamond) among the clathrates we consider, its absolute stability (relative to diamond) is comparable to that of fullerene. The optimized C−C bond lengths are all equal to 1.55 Å, just slightly longer than the ideal 1.54 Å bond length in diamond. The strain is hence mostly induced by the distorted tetrahedral coordination for each C atom in the structure, or, alternatively, by the 90 and 120° angles of the 4- and 6-membered rings composed of sp^3 carbons.

The band structure of Clathrate VII is shown in Figure 2, and the corresponding density of states (DOS) in Figure 3a.

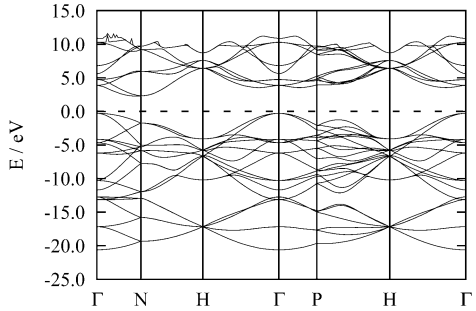

Figure 2. Band structure of Clathrate VII, all carbon. The position of the highest occupied crystal level is indicated by the dashed line.

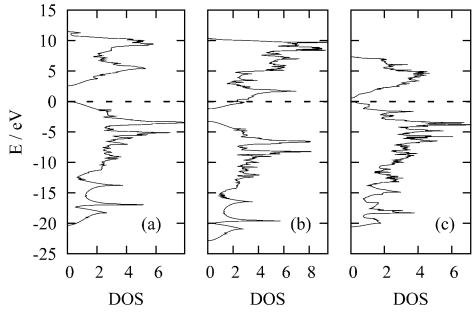

Figure 3. Densities of states of (a) Clathrate VII, (b) $2Li@C_{12}$, and (c) the representative $P4_2/mmc$ $2Li@C_{10}B_2$. The DOS unit is states/eV/unit cell.

Clearly, Clathrate VII is a semiconductor/insulator, with a 2.6 eV indirect band gap between Γ and N. The band gap is enlarged to 3.6 eV with the more reliable non-iterative GW method[69−71] (so-called "one-shot" G0W0). A substantial band gap is expected, as all C atoms form four single bonds and satisfy the octet rule. Our calculated band gap is significantly smaller than the value (5.6 eV) presented in ref 18, very likely for using plane wave basis set here versus atomic basis set there, while the calculated radii of the C_{24} cage are in good agreement (2.45 Å here vs 2.44 Å in ref 18).

Stuffing Li Atoms into Clathrate VII. With this preliminary understanding of Clathrate VII, we proceed to place two Li atoms into the two cavities of each unit cell of this clathrate. In this $2Li@C_{12}$, the symmetry of the lattice is retained. The doping swells the cage, as the C−C bond lengths are increased from 1.55 to 1.59 Å and the $[4^6 6^8]$ polyhedron radius from 2.45 to 2.52 Å. Correspondingly, the unit cell volume increases from 84.3 to 91.4 $Å^3$.

What characteristic size parameters should we use to reach a decision on whether there is or is not room for a Li inside a clathrate cage? Should it be ionic, covalent, or van der Waals

DOI: 10.1021/jacs.5b07883
J. Am. Chem. Soc. 2015, 137, 12639−12652

radii, cognizant of the ambiguity of each? Certainly not covalent/atomic radii, since there cannot be 24 Li−C bonds in each cage. A reasonable compromise, given the prospective charge transfer from Li, in a delocalized way, to the clathrate framework, might be the van der Waals radius of C (1.77 Å[72]) and the cationic radius of Li (0.76 Å[73]). This combination of van der Waals radii and ionic radii for clathrate and guest atoms was used by Karttunen, Fässler, et al. in judging the space needed for encapsulating a guest atom in a cavity.[18] The summation of the two radii (2.53 Å) is not much bigger than the radius of the empty cavity (2.45 Å). Actually, if Bondi's[74] or Batsanov's[75] van der Waals radius of C (1.70 Å) is used, the radii summation (2.46 Å) is about the same as the empty cavity radius. Therefore, the swelling cannot be straightforwardly ascribed to not having enough space in the cavity.

Figure 3b shows the DOS of 2Li@C_{12}; the underlying band structure is shown in Figure S1. Comparing it with Figure 3a, one can see that the two electronic structures are similar, except there are more states on the top of the conduction band in Figure 3b, as one might expect from the extra Li orbitals. The essential difference is the position of the Fermi level (in general, and fully aware of the correct definition of a Fermi level, we loosely call the energy of the highest occupied crystal level the Fermi level in this paper, regardless of whether the material is semiconducting or metallic)—for 2Li@C_{12}, it enters the bottom of the conduction band. The two doped Li atoms lose two electrons which then occupy the orbitals unfilled in the clathrate. Given the octet, diamond-like closed-shell structure of C Clathrate VII, those virtual orbitals must have C−C antibonding character. Their occupation naturally lengthens the C−C bonds and swells the cavity.

Let's look at the bonding character of the states around the Fermi level. This is best done with the Crystal Orbital Hamilton Population (COHP) of Dronskowski and Blöchl.[76] In Figure 4 we plot the COHP between two adjacent C atoms

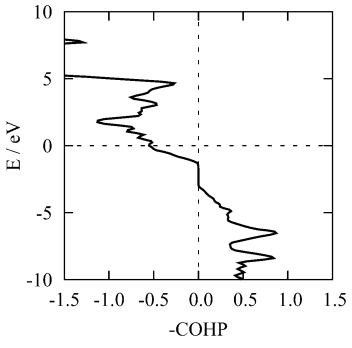

Figure 4. Crystal Orbital Hamilton Population between two adjacent C atoms in 2Li@C_{12} around the Fermi level. The position of the highest occupied crystal level is indicated by the horizontal dashed line. Note that we plot the negative of COHP, following the convention of the chemical community.

in 2Li@C_{12}. The antibonding character of the energy levels around the Fermi level is unambiguous, given the positive COHP there. This statement is supported by the orbital electronic density (the square of the crystal orbital) of the highest occupied crystal orbital (HOCO) of 2Li@C_{12} at the N point of the first Brillouin zone (FBZ).[77] The orbital density is shown in Figure S2; while the density does not show directly the change of phase of the orbital we expect along the CC bonds, indirectly the absence of density at the CC midpoints hints at nodes there. The HOCO there looks identical to the lowest unoccupied crystal orbital (LUCO) of Clathrate VII, which is not shown. For comparison, the HOCO of Clathrate VII is also shown in Figure S2—it displays clear C−C bonding character.

The Zintl picture[78,79] of nearly complete metal-to-nonmetal electron transfer is applicable to 2Li@C_{12}.

What about the energetics of inserting the Li atoms into the C clathrate lattice? As expected, the Li doping is highly endothermic:

$$2\mathrm{Li(bcc)} + \mathrm{C_{12}(Clathrate\ VII)} = 2\mathrm{Li@C_{12}}$$
$$\Delta H = 2.66\ \mathrm{eV/Li} \qquad (2)$$

Overall, the Li metal bonding is disrupted and the C−C bonds of the clathrate are weakened, explaining the increase of enthalpy. Putting 2Li (gas) on the left-hand side, i.e., subtracting the cohesive energy of Li, gives ΔH = 1.01 eV/Li, still an endothermic process.

To summarize, on doping 2 Li atoms into Clathrate VII, we effectively have $2Li^+@C_{12}^{2-}$. While the Li^+ ions fit in sterically, electron occupation of the antibonding orbitals of the clathrate framework exacts a high price, energetically and structurally, for the insertion. Note that two factors would make 2Li@E_{12} (E = Si, Ge, Sn) much happier—a larger cage and a lower energy of the E-E σ^* levels.

Boron Substitution Is a Great Improvement. Given the electronic structure of 2Li@C_{12}, if we can "remove" the two extra high-energy electrons by substituting two C atoms with B (or one C with Be, a substitution not tried here), then we can have a structure that is isoelectronic to Clathrate VII, and possibly more stable. We call this class of double Li-doped, double-B-substituted structures generally 2Li@$C_{10}B_2$. There are in total five symmetrically unique ways to make a double boron substitution in Clathrate VII. Hidden here is an assumption that the substitution retains Z = 1, the same unit cell size. One of the five ways has two adjacent B atoms and we guess the resultant structure should be the least stable. This is because the B is formally negatively charged (B^-). Putting two formally negatively charged sites adjacent to each other is electrostatically unfavorable, and it has been observed that substituted Group 13 atoms in Group 14 clathrates avoid homonuclear bonds.[80,81]

All five optimized 2Li@$C_{10}B_2$ unit cells are shown in Figure 5, with their relative enthalpies and space group symbols. The *Amm*2 structure with adjacent B atoms is the least stable, as expected, by 0.94 eV/unit cell relative to the most stable $P4_2/mmc$ structure. The $P4_2/mmc$, *P*4/*nmm*, and *Ama*2 structures are within 0.40 eV/unit cell in enthalpy.

Can we predict which 2Li@$C_{10}B_2$ isomer would be made; in particular, will it be the $P4_2/mmc$ structure? If only it were as easy as looking at the enthalpies! It is not. The structures in Figure 5a−c are not significantly different in enthalpy. In the real world, kinetics may be at work, and we do not know what method will eventually be found to make these. Once made, a metastable isomer would have a large barrier to rearrange to a more stable form. We are here more in the realm of organic chemistry—the universe of thermodynamically unstable but kinetically persistent molecules—than in high-temperature inorganic chemistry.

Let's examine further the $P4_2/mmc$ structure, most stable in the group, just to have a focus for further analysis. The optimized $P4_2/mmc$ 2Li@$C_{10}B_2$ unit cell has Li at the center of

DOI: 10.1021/jacs.5b07883
J. Am. Chem. Soc. 2015, 137, 12639−12652

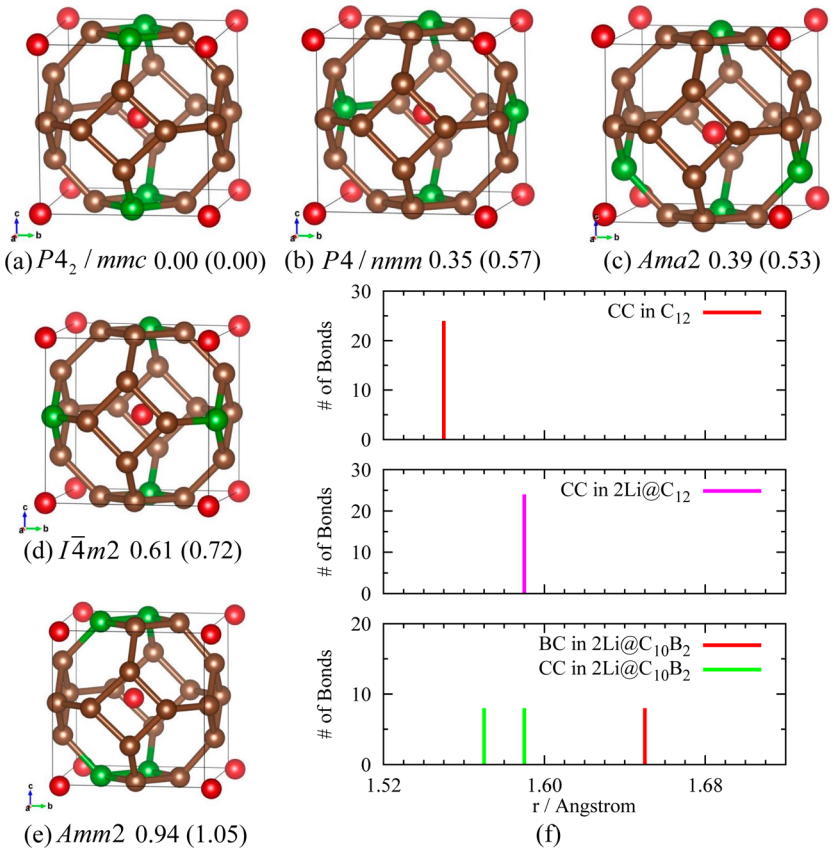

Figure 5. (a)−(e) The five $2Li@C_{10}B_2$ unit cell structures with their relative enthalpies with respect to (a) (eV per unit cell, values in parentheses are under P = 40 GPa) and space group symbols. Li, C, and B are represented by red, brown, and green spheres, respectively. (f) Histograms of B−C and C−C bond lengths in the unit cells of Clathrate VII, $2Li@C_{12}$, and structure (a).

its cavities. The distances from the central Li to the C vertices range from 2.46 to 2.60 Å, while that to the B vertices is 2.54 Å. The 92.9 Å^3 volume of the $2Li@C_{10}B_2$ unit cell, in comparison to the 84.3 Å^3 of Clathrate VII, indicates an even more substantial swelling of the cavity, compared to the 91.4 Å^3 unit cell volume of $2Li@C_{12}$. However, the swelling is more related to the longer C−B bond (1.65 Å in the $P4_2/mmc$ structure, which is consistent with experimental C(sp^3)−B(sp^3) bond lengths in a variety of organoborates[60−62]) than the C−C bonds (1.55 Å in Clathrate VII), instead of occupying antibonding orbitals of the clathrate framework. From Figure 5f, a histogram of distances, we can clearly see the C−C bond length elongation on Li insertion and the re-contraction of some of the C−C bonds after B substitution, removing the corresponding antibonding character.

On doping two borons into the carbon framework, the semiconductor nature of the parent clathrate is restored. The DOS of the $P4_2/mmc$ $2Li@C_{10}B_2$ isomer is shown in Figure 3c; the corresponding band structure is in Figure S3. Although the symmetry is lowered from $Im\bar{3}m$ of $2Li@C_{12}$, the two systems share similar features within the valence and conduction bands, respectively, and the indirect band gap also occurs between Γ and N. The similar electronic structures in the valence bands confirm that $2Li@C_{10}B_2$ should be viewed as $2Li^+@C_{10}B_2^{2-}$.

In $P4_2/mmc$ $2Li@C_{10}B_2$, there are three unique adjacent atomic pairs, corresponding to a C−B (1.65 Å) and two C−C (1.57 and 1.59 Å) bonds. COHPs of the three bonds are shown in Figure S4. Only a few C−C antibonding states remain just below the HOCO.

To a reasonable approximation, the plan of not occupying antibonding orbitals through B substitution seems to work.

Despite the similarity of their electronic structures, $P4_2/mmc$ $2Li@C_{10}B_2$ features a smaller band gap than Clathrate VII: 0.6 vs 2.6 eV (1.3 vs 3.6 eV with the G0W0 method); see Figure 3c. The lower electronegativity of B and the negatively charged framework push up the energies of the valence band to be close to the conduction band. $2Li@C_{10}B_2$ should be a good semiconductor. Note that Li-doped, B-substituted Si clathrates were also predicted to be good semiconductors.[51,82]

What about thermodynamic stability? For the following reaction,

$$2Li(bcc) + 2B(\alpha\text{-}B_{12}) + C_{12}(\text{Clathrate VII}) = 2Li@C_{10}B_2(P4_2/mmc) + 2C(\text{diamond}) \quad (3)$$

the calculated reaction enthalpy is −0.16 eV/Li. The energy costs in breaking the Li metal and B−B multicenter bonds in the elemental structures are compensated by the Coulombic interaction between the Li cations and the negatively charged $C_{10}B_2$ framework, as well as the formation of the more stable (over Clathrate VII) "extruded" C in the diamond structure. To get a feeling for the importance of the formation of diamond, we tried to formulate the formation reaction without explicit involvement of diamond, as follows:

$$2Li(bcc) + 2B(\alpha\text{-}B_{12}) + \frac{5}{6}C_{12}(\text{Clathrate VII}) = 2Li@C_{10}B_2(P4_2/mmc) \quad (4)$$

DOI: 10.1021/jacs.5b07883
J. Am. Chem. Soc. 2015, 137, 12639−12652

The reaction (formation) enthalpy is 0.22 eV/Li; diamond formation, or, to put it in other words, the strong cohesive energy of diamond, switches the doping-and-substitution process from endothermic to exothermic. Although the reaction enthalpy of eq 3 is evaluated at 1 atm, we choose diamond, instead of graphite, as the C reference. The reason for this is that the C atoms in clathrates are approximately tetrahedral and we would like to maintain this geometry/hybridization on the two sides of the equation. Since graphite and diamond are so close in enthalpy (graphite lower by 0.02 eV/C),[83] replacing diamond by graphite would not result in any qualitative change of the formation enthalpy.

One way or the other, there is great stabilization upon B substitution. Compared to the 2.66 eV/Li doping enthalpy mentioned above for 2Li@C_{12}, $P4_2/mmc$ 2Li@$C_{10}B_2$ should be (thermodynamically) easier to synthesize.

Li Doping and B Substitution under Elevated Pressure. In recent work by one of us (Strobel et al.), a novel Si clathrate allotrope, Si_{24}, was made by synthesizing Na_4Si_{24} under pressure,[84] followed by removal of the Na by heating and lowering the pressure.[85] So pressure is naturally on our minds as we think about the Li-doped carbon clathrates.

Considering the change of volume in the Li doping and B substitution in Clathrate VII (−17.7 Å^3/Li for the reaction in eq 3 at P = 1 atm), the synthesis of the 2Li@$C_{10}B_2$ is expected to be more favorable under high pressure. Indeed, the calculated reaction enthalpy for the following formula,

$$2\mathrm{Li(cI16)} + 2\mathrm{B}(\gamma\text{-}\mathrm{B}_{28}) + \mathrm{C}_{12}(\text{Clathrate VII}) = 2\mathrm{Li@C_{10}B_2}(P4_2/mmc) + 2\mathrm{C(diamond)} \quad (5)$$

at P = 40 GPa is −2.61 eV/Li. That is a 2.45 eV/Li greater (than at P = 1 atm) exothermicity for the reaction. Note that the most stable phases of Li[86] and B[87] under this pressure are chosen to calculate the enthalpy. 40 GPa is not difficult to reach with today's technology, and the significantly more negative doping−substitution enthalpy is a promising sign for prospective synthesis of 2Li@$C_{10}B_2$.

The order of the stabilities of the five isomers is roughly maintained as the pressure is raised to 40 GPa. The calculated 1 atm unit cell volumes of the five 2Li@$C_{10}B_2$ isomers are 92.9, 94.0, 93.6, 93.5, and 93.4 Å^3, in the order of Figure 5a−e, so the increasing stabilization of the first, the $P4_2/mmc$ 2Li@$C_{10}B_2$ structure is not unexpected. But there is no clear effect otherwise of unit cell volume at 1 atm.

Clathrate I: Easier To Encapsulate Li in Smaller Cavities? Alkaline-metal-filled Group 14 Clathrates I of Si, Ge, and Sn entered the sight of scientists about 50 years ago,[42,88] and have remained central to the field since then.[89] Still, no carbon Clathrate I, filled or unfilled, has been synthesized. The 46-atom unit cell of Clathrate I is made up of two [5^{12}] and six [$5^{12}6^2$] polyhedra (see Figure 1a), with C atoms occupying the 24*k*, 16*i*, and 6*c* Wyckoff sites of the $Pm\bar{3}m$ space group. The various sites are marked in three colors in Figure 6. Each [5^{12}] cage contains 12 24*k* and 8 16*i* Wyckoff sites, while each [$5^{12}6^2$] cage contains 12 24*k*, 8 16*i*, and 4 6*c* sites.

There are in total four types of C−C bonds, between C atoms at the16*i* and 16*i*, 16*i* and 24*k*, 6*c* and 24*k*, and 24*k* and 24*k* sites, respectively. The corresponding bond lengths in our optimized structure are 1.52, 1.54, 1.57, and 1.59 Å. The lower limit (106°) of the CCC bond angle range we find is close to the ideal tetrahedral bond angle 109.5°. The upper limit (124°)

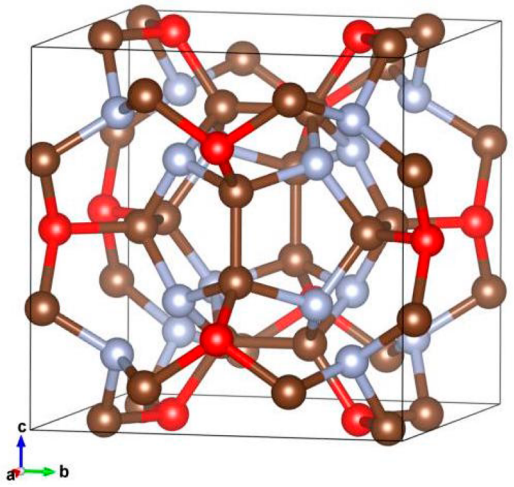

Figure 6. Optimized unit cell structure of C Clathrate I, with the C atoms occupying the 24*k*, 16*i*, and 6*c* Wyckoff sites marked with brown, light blue, and red colors, respectively. It takes a while to see the fragments of the component polyhedra, which were completed in the representation of Figure 1. But they are there.

is clearly related to the 6-membered rings in the [$5^{12}6^2$] polyhedron. Note that the bond lengths of Clathrate I have a broader distribution and larger deviations from the norm of 1.54 Å of diamond than those in Clathrate VII. Yet Clathrate I is more stable than Clathrate VII (relative enthalpies 0.11 vs 0.39 eV/C, Table 1). The indication is that bond angles deviating from ideal tetrahedral coordination contribute more than bond stretches to the strain in the clathrates.

That is not what one might have anticipated from bond stretching and bending force constants. However, using neopentane as a model system, we show in section S2 in the SI that bending the CCC bond angle from 109° to 90° costs almost 0.6 eV, while stretching the C−C bond from 1.54 to 1.64 Å costs only 0.15 eV. Apparently, the magnitude of bending the CCC angle in Clathrate VII to 90° is so large that the harmonic oscillator approximation fails. Thus, predictions based on force constants may not be realistic.

Clathrate I is an insulator or semiconductor. The DOS of this hypothetical yet attractive phase is shown in Figure 7a, the underlying band structure is shown in Figure S7. The 3.9 eV band gap (5.6 eV at the G0W0 level) is larger than the 2.6 eV (3.6 eV) band bap of Clathrate VII, consistent with the former being more stable. Our 5.6 eV G0W0 gap is still lower than the

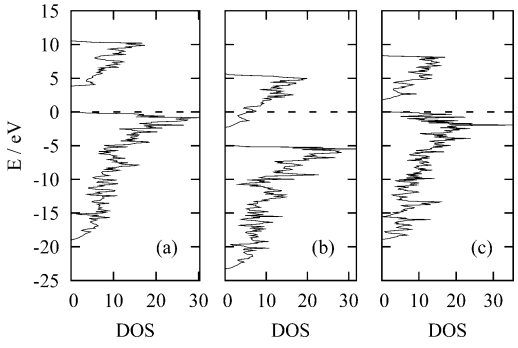

Figure 7. Densities of states of (a) Clathrate I, (b) 8Li@C_{46}, and (c) the representative $R3c$ 8Li@$C_{38}B_8$. The DOS unit is states/eV/unit cell.

DOI: 10.1021/jacs.5b07883
J. Am. Chem. Soc. 2015, 137, 12639−12652

6.2 eV gap reported in ref 18, but close to the 5.3 eV GW gap reported in refs 90 and 91.

Doping eight Li atoms per unit cell in Clathrate I, i.e., filling all its cavities, increases the unit cell volume from 300.9 to 319.3 Å^3. As mentioned in the beginning of the paper, this full doping costs 2.31 eV/Li enthalpy. Isn't it strange? The cavity in Clathrate VII is larger than those in Clathrate I (radii 2.45 vs 2.17 and 2.41 Å, Table 1), but it costs more in enthalpy to fully dope Li in the former (2.66 vs 2.31 eV/Li in enthalpy). Apparently, cavity size is not the only thing that matters.

In Clathrate I, further calculations of partial doping indicate that it takes 2.85 eV/Li to dope two Li atoms in the two small [5^{12}] cavities, and 2.21 eV/Li to put in six Li atoms in the six larger [$5^{12}6^2$] cavities in Clathrate I. Thus, within the same clathrate, the cavity size does determine the difficulty of inserting lithiums. The weighted average of the doping enthalpies in the two types of cages, i.e., $(2.85 \times 2 + 2.21 \times 6)/8 = 2.37$ eV/Li, is similar to the 2.31 eV/Li obtained for the fully doped 8Li@C_{46}.

Shown in Figure 7b is the DOS of 8Li@C_{46}; the band structure is shown in Figure S7. Comparing parts (a) and (b) in Figure 7, we again see signs of electron transfer, filling the antibonding levels of the C framework. The COHPs in Figure 8

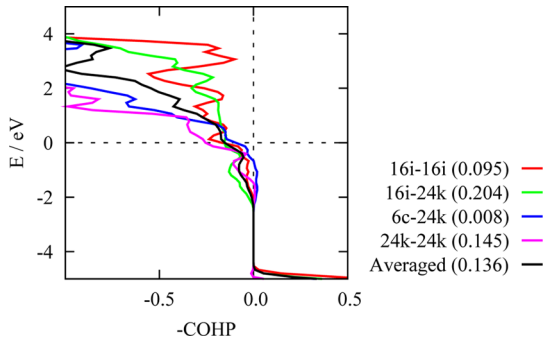

Figure 8. Crystal Orbital Hamilton Populations of the four types of C−C bonds and their weighted average in 8Li@C_{46} around the Fermi level. The position of the highest occupied crystal level is indicated by the horizontal dashed line. The numbers in parentheses are the integrated COHP (in eV) from $E = -4$ to 0 eV. Note that we plot the negative of COHP, following the convention of the chemical community.

show that the levels below the Fermi level are C−C antibonding, but more weakly so than for Clathrate VII. The reason for the smaller doping enthalpy of 8Li@C_{46} now becomes clear: the orbitals that accept the Li electrons are less antibonding in 8Li@C_{46} than in 2Li@C_{12}. Underlying this comparison is the commensurate increase of the number of C atoms (and C−C bonds: from 12 to 46 atoms and from 24 to 96 bonds, about 4-fold) and the number of cavities (and antibonding electrons coming from Li) from 2 to 8, 4-fold) per unit cell as the clathrate is changed from Type VII to I. The weaker antibonding character in 8Li@C_{46} is quantitatively justified by the its less positive averaged integrated COHP of the orbitals occupied in the Li insertion, 0.136 eV (Figure 8), compared to the 0.417 eV counterpart of 2Li@C_{12} (obtained in a similar way, using the COHP in Figure 4).

Boron Substitution Strategies. We want to replace 8 out of 46 carbons with borons, so as to balance the charge if the Li change to Li^+, as they must. There is no way we can examine all the structures—the combinatorial possibilities are too large. What strategies might we come up with to delimit the set of isomers to be considered?

1. *Symmetry*. Nature seems to favor a medium reduction in symmetry. So there are bent as well as linear ABA molecules, but as a first approximation no ABA molecules with unequal bond lengths.[92] So we could examine for 8Li@$C_{38}B_8$ those isomers with the largest possible subgroups of the cubic $Pm\bar{3}n$, the space group of Clathrate I.
2. *Charge*. The three distinct Wyckoff sites of Clathrate I bear different charges. If we integrate the projected DOS up to the HOCO level, we get populations of 4.02, 3.97, and 4.01 valence electrons for the C atoms at the 24*k*, 16*i*, and 6*c* sites. A simple electronegativity argument would argue for B substitution at the sites bearing less electron population, i.e., the 16*i* site.
3. *Bonding*. As the COHP values of Figure 8 show, some bonds just below the Fermi level of 8Li@C_{46} are weakened more than others. Why not substitute B in those bonds, to avoid occupying those antibonding levels?
4. *Stress relief*. The 6*c* sites in Clathrate I are common vertices of two 6-membered rings, and thus feature two bond angles close to 120°, substantially different from the ideal 109.5° bond angles of a four-coordinated C. We expect some bond angle stress.[51] B substitutions on those sites can reduce this stress, and this is shown using a $B(CH_3)_4^-$ model in the SI, section S2. Actually, Group 13 substitutions in 8K@Ga_8Sn_{38}, 8Rb@Ga_8Sn_{38}, and 8Rb@Ga_8Ge_{38} primarily occur on the 6*c* sites.[49,50]

We tried all four approaches: the gruesome details are given in section S4 in the SI. The stress relief strategy appears most successful, leading to the lowest enthalpy structures. A representative *R*3*c* 8Li@$C_{38}B_8$ unit cell obtained following this strategy, with all 6*c* and two 16*i* sites substituted by B atoms, is shown in Figure 9a, with the statistics of the bond lengths in the unit cell in Figure 9b. Comparing the bond lengths in Clathrate I, 8Li@C_{46}, and 8Li@$C_{38}B_8$ in Figure 9b, the trend is apparent: Li doping stretches the C−C bond lengths significantly, reflecting the aforementioned effect of filling C−C antibonding orbitals. The subsequent B substitution re-contracts some of the C−C bonds, stabilizing the structure. This is similar to the case of Clathrate VII (Figure 5d) discussed above.

The *R*3*c* 8Li@$C_{38}B_8$ structure we have discussed has the lowest enthalpy among all 8Li@$C_{38}B_8$ structures that we have explored (see section S4 in the SI for all of them). But, it is not substantially lower in enthalpy: some other isomers are just 0.005 eV/Li higher. We think that when an 8Li@$C_{38}B_8$ solid will be made, it is likely to be an unpredictable mixture of substitutional isomers, potentially an amorphous solid.

The calculated DOS of the *R*3*c* 8Li@$C_{38}B_8$ is shown in Figure 7), band structure given in Figure S7. There is now a 1.8 eV band gap (2.9 eV at the G0W0 level). As we expected, *R*3*c* 8Li@$C_{38}B_8$ is calculated to be a semiconductor. With the degeneracy lifting due to the lower symmetry (*R*3*c* vs $Pm\bar{3}n$), the bands (see Figure S7) still show the tendency to merge at the R point, which is a sign of similar band structures of the 8Li@$C_{38}B_8$ and Clathrate I structure. The smaller band gap of the 8Li@$C_{38}B_8$ (1.8 vs 3.9 eV of Clathrate I (2.9 vs 5.9 eV at the G0W0 level)) should again be attributed to the negatively

DOI: 10.1021/jacs.5b07883
J. Am. Chem. Soc. 2015, 137, 12639−12652

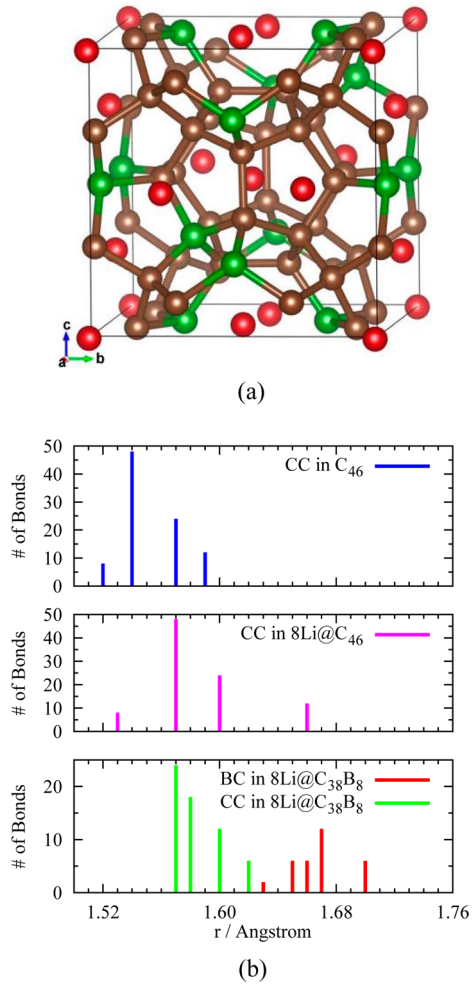

Figure 9. (a) Optimized *R*3*c* 8Li@$C_{38}B_8$ unit cell with six 6*c* and two 16*i* carbon atoms substituted by B. (b) Histograms of B−C and C−C bond lengths in the unit cells of Clathrate I, 8Li@C_{46}, and structure (a). Li, C, and B are represented by red, brown, and green spheres, respectively. The binning resolution in (b) is 0.01 Å.

charged framework and the lower electronegativity of B compared to C.

The calculated reaction enthalpy for the Li doping and B substitution, i.e.,

$$8\mathrm{Li(bcc)} + 8\mathrm{B}(\alpha\text{-}\mathrm{B}_{12}) + \mathrm{C}_{46}(\text{Clathrate I}) = 8\mathrm{Li@C}_{38}\mathrm{B}_8(R3c) + 8\mathrm{C(diamond)} \quad (6)$$

is 0.12 eV/Li. One contribution to this larger and positive value (vs −0.16 eV/Li reaction enthalpy of the similar process of Clathrate VII) is the stability of Clathrate I (0.28 eV/C more stable than Clathrate VII, see Table 1).

At P = 40 GPa, the reaction enthalpy for

$$8\mathrm{Li(cI16)} + 8\mathrm{B}(\gamma\text{-}\mathrm{B}_{28}) + \mathrm{C}_{46}(\text{Clathrate I}) = 8\mathrm{Li@C}_{38}\mathrm{B}_8(R3c) + 8\mathrm{C(diamond)} \quad (7)$$

is calculated to be −2.18 eV/Li. Again, the volume reduction of Li doping and B substitution (−16.4 Å^3/Li for eq 6) favors the formation of 8Li@$C_{38}B_8$ at high pressure.

We proceed to an abbreviated discussion of Clathrates IV, H, and II; more details are provided in sections S5−S7 in the SI.

Clathrate IV: B Substitutions Motivated by Relief of Both Bond Angle Stress and Bond Length Elongation. Clathrate IV has six fewer atoms than Clathrate I, and one fewer cage in the unit cell. It is also called hex-C_{40} and was first proposed theoretically in 1995.[93] There was a study on doping Li and substituting B for C, separately, for this clathrate,[94] but the two perturbations were not tried together. There are three [5^{12}], two [$5^{12}6^2$], and two [$5^{12}6^3$] polyhedra in its unit cell (see Figure 1c), and they are composed of C atoms at the 12*n*, 6*m*, 12*o*, 6*j*, and 4*h* Wyckoff sites of the *P*6/*mmm* space group. Our optimized hexagonal unit cell structure of Clathrate IV is shown in Figure 10.

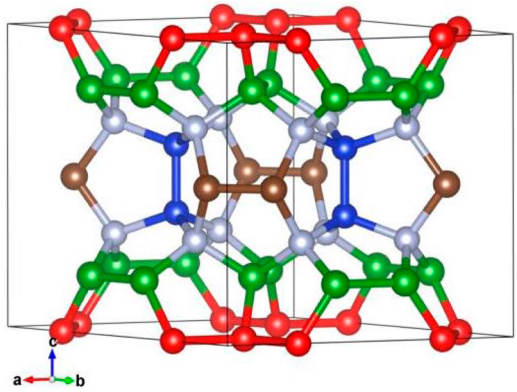

Figure 10. Optimized unit cell structure of C Clathrate IV, with the C atoms occupying the 24*n*, 6*m*, 12*o*, 6*j*, and 4*h* Wyckoff sites marked with green, brown, light blue, red, and blue colors, respectively.

There are eight types of C−C bonds in the unit cell with the following bond lengths: 1.51 Å for 12*o*-4*h*, 1.52 Å for 4*h*-4*h*, 1.53 Å for 6*m*-6*m*, 1.54 Å for 12*n*-12*o*, 1.56 Å for 12*o*-6*m*, 1.57 Å for 12*n*-6*j*, 1.63 Å for 12*n*-12*n*, and 1.66 Å for 6*j*-6*j*. With many bonds longer than the diamond norm (1.54 Å) by more than 0.1 Å, Clathrate IV is still fairly stable, with 0.13 eV/C relative enthalpy (Table 1) compared to diamond. We think this is quite remarkable—organic molecules with such long bonds are found only in a small number of strained molecules.[95] Similar bond elongation also occurs in Si Clathrate IV: the longest Si−Si bond in our optimized structure is 2.47 Å between the two 6*j*-6*j* sites, 0.13 Å longer than the bond in the Si diamond-like crystal. Clathrate IV is, as expected, a semiconductor (see section S5 in the SI for more discussion).

Li insertion costs energy, as expected. As the detailed discussion in section S5 of the SI shows, the long 6*j*-6*j* and 12*n*-6*j* bonds are even longer in 7Li@C_{40}, consistent with their most significant gains of antibonding character (the most positive incremental COHP values (Figure S13)) in the insertion.

Detailed in section S5 in the SI is also how we came to the B substitution pattern on three 6*j*, two 12*n*, and two 4*h* sites. With those substitutions, the number of 6*j* C atoms that are shared vertices of two 6-membered rings is halved, and the numbers of the stretched 12*n*-12*n* and 4*h*-4*h* C−C bonds are reduced. The resulting (we think representative) *C*2 7Li@$C_{33}B_7$ has its unit cell shown in Figure 11.

The doping and substitution reaction,

$$7\mathrm{Li(bcc)} + 7\mathrm{B}(\alpha\text{-}\mathrm{B}_{12}) + \mathrm{C}_{40}(\text{Clathrate IV}) = 7\mathrm{Li@C}_{33}\mathrm{B}_7(C2) + 7\mathrm{C(diamond)} \quad (8)$$

DOI: 10.1021/jacs.5b07883
J. Am. Chem. Soc. 2015, 137, 12639−12652

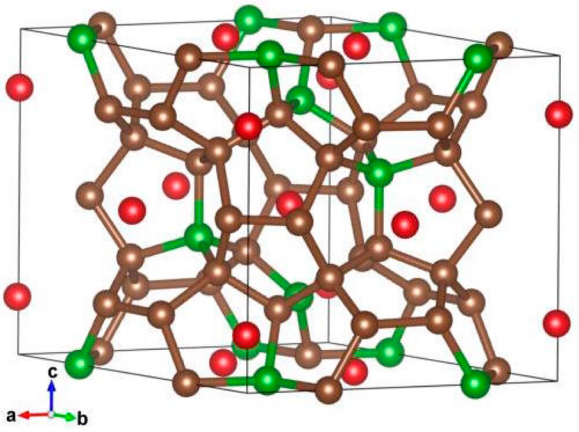

Figure 11. Optimized unit cell structure of the representative *C*2 7Li@$C_{33}B_7$. Li, C, and B are represented by red, brown, and green spheres, respectively.

costs 0.32 eV/Li in enthalpy. At P = 40 GPa, the reaction enthalpy for the following reaction,

$$7\mathrm{Li(cI16)} + 7\mathrm{B}(\gamma\text{-}\mathrm{B}_{28}) + \mathrm{C}_{40}(\text{Clathrate IV}) = 7\mathrm{Li@C}_{33}\mathrm{B}_7(C2) + 7\mathrm{C(diamond)} \quad (9)$$

is −1.91 eV/Li. The volume change for reaction in eq 8 is −15.6 Å^3/Li at 1 atm, and this value changes little from eq 3 (−17.7 Å^3) to eq 6 (−16.4 Å^3), and to eq 8. That makes perfect sense, as the most significant volume change comes from the release of the volume taken by Li solid, which is about 20 Å^3/Li in the bcc crystal.

Clathrate H: Less Room for Lithiums. Although they share the same *P*6/*mmm* space group symmetry, Clathrate H has six fewer C atoms and correspondingly one fewer cage in its unit cell than Clathrate IV (see Figure 1e and Table 1). Our optimized Clathrate H unit cell is shown in Figure 12. It

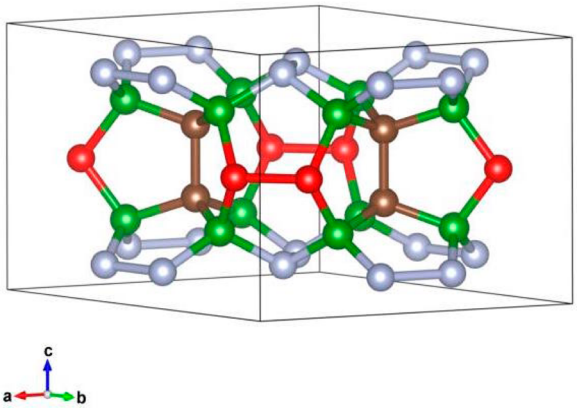

Figure 12. Optimized unit cell structure of C Clathrate H, with the C atoms occupying the 12*o*, 4*h*, 12*n*, and 6*i* Wyckoff sites marked with green, brown, light blue, and red, respectively.

features four types of occupied Wyckoff positions and seven types of C−C bonds: 1.53 Å for 4*h*-4*h*, 1.54 Å for 12*n*-12*o*, 1.55 Å for 12*o*-4*h*, 1.56 Å for 6*i*-6*i*, 1.56 Å for 12*n*-12*n* ($\|_c$), 1.57 Å for 12*n*-12*n* ($\perp_c$), and 1.57 Å for 12*o*-6*i*. The 12*o* C atoms are grouped into three squares in the unit cell and thus there are two types of perpendicular 12*n*-12*n* bonds, the ones that are perpendicular to the *c*-axis (labeled as $\perp_c$ and shown as the light blue bonds in Figure 12) and the ones that are parallel to the *c*-axis (labeled as $\|_c$). (Since only bonds that are completely contained in the unit cell are shown in the figure, the 12*n*-12*n* ($\|_c$) bonds cannot be seen in Figure 12. They are more clearly displayed in Figure 1e.)

Despite the cyclobutane-like squares in its structure (90° bond angles), Clathrate H is only 0.14 eV/C higher in enthalpy than diamond, significantly more stable than Clathrate VII. One obvious reason is that every C vertex in Clathrate VII has two 90° bond angles, while only 12 (out of 34) in the Clathrate H unit cell have one 90° bond angle each.

It takes 2.30 eV/Li to fully dope six Li atoms into the clathrate. Section S6 in the SI has a detailed analysis of the consequences, and follows through with a B substitution strategy based on relief of bond angle stress and bond length modification ensuing from hypothetical Li doping. Six 12*n* C atoms are substituted. In addition to the stress and stretch, enlarging the small [$4^3$5^{6}6^3] cage (with the shortest 2.03 Å center-to-cage minimum distance in Table 1) is a hidden motivation for this substitution. A representative isomer of $P\bar{3}1m$ symmetry is shown in Figure 13. There are other isomers, close in enthalpy.

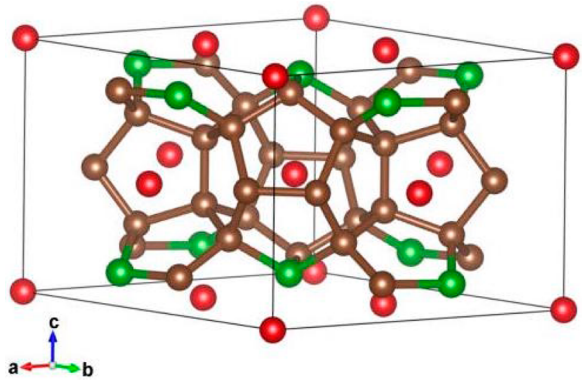

Figure 13. Optimized unit cell structure of the representative $P\bar{3}1m$ 6Li@$C_{28}B_6$. Li, C, and B are represented by red, brown, and green spheres, respectively.

The reaction enthalpy for the Li doping and B substitution reaction,

$$6\mathrm{Li(bcc)} + 6\mathrm{B}(\alpha\text{-}\mathrm{B}_{12}) + \mathrm{C}_{34}(\text{Clathrate H}) = 6\mathrm{Li@C}_{28}\mathrm{B}_6(P\bar{3}1m) + 6\mathrm{C(diamond)} \quad (10)$$

is calculated to be 0.51 eV/Li. At P = 40 GPa, as anticipated, the reaction enthalpy for

$$6\mathrm{Li(cI16)} + 6\mathrm{B}(\gamma\text{-}\mathrm{B}_{28}) + \mathrm{C}_{34}(\text{Clathrate H}) = 6\mathrm{Li@C}_{28}\mathrm{B}_6(P\bar{3}1m) + 6\mathrm{C(diamond)} \quad (11)$$

becomes exothermic, by −1.79 eV/Li.

Clathrate II: Most Stable, Least Stabilized. Clathrate II, a common structure for other nodes,[96,97] has for carbon the lowest relative enthalpy with respect to diamond, as shown in Table 1. The discussion here is abbreviated (see section S7 in the SI for further details), as many of the points parallel what we have found for the other clathrates.

The conventional unit cell of the $Fd\bar{3}m$ structure has 136 atoms, posing a computational problem. But the 34-atom primitive unit cell is tractable. As Table 2 and previous work[18]

DOI: 10.1021/jacs.5b07883
J. Am. Chem. Soc. 2015, 137, 12639−12652

by others indicate, this is the lowest enthalpy pure C alternative to diamond among the clathrates, for the bond length and angle adjustments to the strain of filling space are smallest. Li doping into the $[5^{12}]_4[5^{12}6^4]_2$ polyhedra of the structure is accomplished with moderate repulsion (see Table 2); the $[5^{12}]$ cages are small, but the $[5^{12}6^4]$ ones are relatively roomy.

A variety of strategies for B doping were tried. There are many competitive structures; the lowest enthalpy (by a little) one we have found is the *P*1 structure shown in Figure 14.

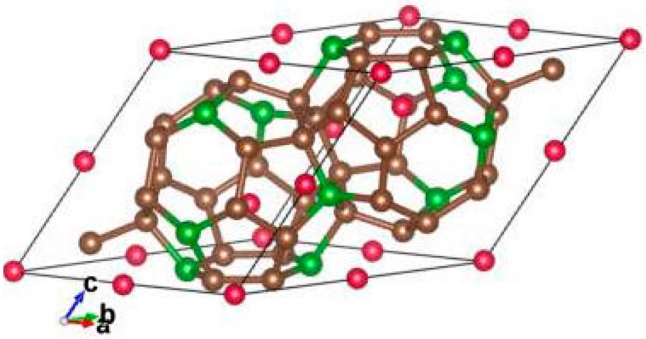

Figure 14. Optimized structure (in a rhombohedral primitive unit cell) of a *P*1 B-substituted $6Li@C_{28}B_6$ Clathrate II structure.

The signs of stabilization on B substitution are all there (see SI), in "renormalization" of distances, and in enthalpy. The calculated reaction enthalpy for

$$6Li(bcc) + 6B(\alpha\text{-}B_{12}) + C_{34}(\text{Clathrate II}) = 6Li@C_{28}B_6(P1) + 6C(\text{diamond}) \quad (12)$$

is 0.52 eV/Li. At P = 40 GPa (different structures for Li and B) it becomes −1.73 eV/Li. The two reaction enthalpies are the highest (least negative) among all five clathrates considered; Li insertion and B substitution brings the least stabilization, in accord with the most stable clathrate coming on the left-hand side of the reaction formula.

Trying To Stuff Diamond with Lithiums. The diamond "cavity" is tiny, with a 1.68 Å radius.[98] Not surprisingly, trying to fill every cavity with Li leads in theory to disruption of the lattice, with resultant C−C distances >3 Å. If we then try our strategy of compensating B atoms, since the initial stoichiometry is LiC, we reach LiB, all carbons gone. Remarkably, a material of this stoichiometry exists![99−101] At P = 1 atm, LiB features B needles (a *karbin* analogue). At the higher pressure of 40 GPa, LiB is predicted to have a graphitic layer-type structure, and eventually, above 80 GPa, a stuffed NaTl diamondoid structure.[99]

Competition: LiBC and Vacancies. Two competing channels for $xLi@C_yB_x$ synthesis come to mind. The first is the formation of LiBC, a known stable phase.[102] Taking the Li-doped, B-substituted Clathrate I structure for example, the calculated reaction enthalpy for

$$8LiBC(P6_3/mmc) + 30C(\text{diamond}) = 8Li@C_{38}B_8(R3c) \quad (13)$$

is +2.01 eV at P = 1 atm and +1.81 eV at P = 40 GPa. Here we have assumed that LiBC maintains its stoichiometry and space group symmetry at the higher pressure. Relaxation of this assumption simply makes the reaction more endothermic. One should thus avoid pathways that involve LiBC in synthetic attempts directed at Li-doped, B-substituted C clathrates. In clathrate formation, kinetic factors and space filling are likely to play important roles, beyond thermodynamics. If there is a local minimum on the potential energy surface, it may be accessible through fast topologically directed kinetics and presence of templates, which need some time to segregate away during phase transformation. Thus, in another context, zeolites are thermodynamically less stable than sand, but they are synthesizable and separable. LiBC, featuring a layer structure, should be "kinetically avoidable" from the cage structure of $xLi@C_yB_x$ (layer vs cage, graphite vs diamond).

Another possible channel is the formation of vacancies, instead of B substitutions, on the C sites. Alkali metal-inserted type I clathrates of other Group 14 elements with vacancies are well known, e.g., $8Rb@Sn_{44}\square_2$, $8Cs@Sn_{44}\square_2$, $8K@Ge_{44}\square_2$, and $8A@Sn_{44}\square_2$ (A being a mixture of K and Cs),[103−106] with the vacancies (□) preferentially in the 6*c* sites.

The presumption, based on the above other Group 14 structures, is that each vacancy formally removes a carbon atom. If four electrons per vacancy are added, one has effectively four carbanions, so one needs two C vacancies per eight inserted Li atoms, to formally satisfy the octet structure. The vacancies are places of local electronic stress—the carbanions would be only 2.6 Å apart in unrelaxed structure.

We have calculated several models for $8Li@C_{44}\square_2$; the details are given in section S8 in the SI. The C's surrounding the vacancies become less pyramidal, and move apart, to C−C distances >3 Å. The Li's around these anionic sites move in, in an attempt to stabilize the structure.

It is not easy to calculate the relative energetics of competing formation of vacancies and B substitution. For the vacancy model, we calculate the reaction enthalpy for[107]

$$6C(\text{diamond}) + 8Li@C_{38}B_8(R3c) = 8Li@C_{44}\square_2(Cc) + 8B(\alpha\text{-rhombohedral}) \quad (14)$$

and the result is 1.38 eV/Li; it increases to 1.75 eV/Li at P = 40 GPa and with the 8B taking the most stable phase (γ-B_{28}) at that pressure. Given the kinetic convenience to access boron, the synthesis of $8Li@C_{38}B_8$ (*R*3*c*) should be competitive with vacancy formation.

CONCLUSIONS

In the preceding sections we have given a blow-by-blow description of what transpires when the cavities of five carbon clathrates are first filled by lithiums, and when a corresponding number of borons are then inserted into the clathrate framework, replacing carbons. It is time to summarize the results. In doing so, we de-emphasize the energetically costly Li stuffing. This process is unrealistic, and was just a conceptual step for us, to guide us to a strategy for B substitution. We also reiterate a point we made before: there is absolutely no guarantee that for any $xLi@C_yB_x$ solid we have found the global low-enthalpy isomer. We do believe that the isomers on which we have based our numerical analyses are representative ones.

With this caveat, we present in Table 2 a summary of the important results for $xLi@C_yB_x$, the Li-doped, B-substituted clathrates. The formation enthalpies for those systems are also given in the table, in addition to the Li doping−B substitution enthalpies, since the synthesis pathway is not necessarily through forming C clathrates first and making Li doping and B substitution later. The two enthalpies are connected through the formation enthalpies of the C clathrates and qualitatively

DOI: 10.1021/jacs.5b07883
J. Am. Chem. Soc. 2015, 137, 12639−12652

Table 2. Calculated Properties of the Five Li-Doped, B-Substituted Carbon Clathrates Investigated in This Paper

structure	enthalpy for Li doping and B substitution[a] (eV/Li)	formation enthalpy[b] (eV/Li)	r_{CC} range (Å)	r_{BC} range (Å)	∠ range[c] (°)	band gap[d] (eV)
I, $8Li@C_{38}B_8$	0.12, −2.18	0.74, −0.46	1.57−1.62	1.63−1.70	102−126	1.8, 2.9
II, $6Li@C_{28}B_6$	0.52, −1.73	0.94, −0.15	1.56−1.63	1.63−1.71	104−123	1.1, 2.2
IV, $7Li@C_{33}B_7$	0.32, −1.91	1.06, 0.09	1.54−1.66	1.60−1.80	104−125	1.4, 2.6
VII, $2Li@C_{10}B_2$	−0.16, −2.61	2.15, 1.50	1.57−1.59	1.65	84−122	0.6, 1.3
H, $6Li@C_{28}B_6$	0.51, −1.79	1.27, 0.31	1.53−1.62	1.66−1.69	84−121	1.3, 2.2

[a]Both the enthalpies at P = 1 atm (first) and 40 GPa (second) are given. [b]Both the enthalpies at P = 1 atm (first) and 40 GPa (second) are given. The enthalpies are calculated for the reaction xLi + xB + zC → xLi@C_zB_x, with C always being diamond, Li and B in their respective stable phases at the two pressures, e.g., see eqs 6 and 7. [c]All four types of angles, CCC, CBC, BCB, and CCB, are included; a further breakdown can be found in section S8 in the SI. [d]The two values correspond to the gap extracted from the conventionally calculated DOS and the G0W0 gap.

show the same trend. Since those formation enthalpies of the C clathrates are all positive (relative enthalpies in Table 1), the formation enthalpies in Table 2 are all shifted up compared to the Li doping and B substitution enthalpies. Still, the −0.46 eV/Li formation enthalpy for $8Li@C_{38}B_8$ at P = 40 GPa is encouraging. It would also not be unrealistic to consider beryllium instead of boron substitution at cage positions. This may lead to more local strain but fewer impurity positions in the clathrate structures.

We have in several ways shown that Li-filled, B-substituted clathrates are stabilized:

1. B substitution lowers substantially the enthalpic cost of inserting Li atoms into clathrate cages (compare the last column in Table 1 and the first values of the second columns in Table 2). At P = 1 atm, this stabilization amounts to about −2 eV/Li, and it occurs even for clathrates with small cages that really do not have room for a Li-dopant, e.g., $[5^{12}]$ and $[4^35^66^3]$.
2. The resulting clathrates, for the five cases we have studied, show a reasonable range of C−C and C−B bond lengths, especially in comparison to the Li-doped clathrates without B substitution. The structural features of the clathrates are not altered by Li doping and B substitution, as demonstrated by the similar ranges of bond angles in Tables 1 and 2. Also, all the resulting clathrates display a semiconducting electronic structure. The Li doping−B substitution does reduce their band gaps. Elevated pressure enhances the theoretical stabilization (compare the two values in the second or third column in Table 2).

We have explored a range of strategies for deciding just where, in the clathrates, boron substituents will go—symmetry, charge distribution, strengthening bonding, relieving angle, and distance strain. These ideas lead us to a representative low-enthalpy Li-doped, B-substituted candidate for each type of clathrate we study, but it is apparent that in each case there are several enthalpically competitive structures.

We have also investigated two possible competing channels for xLi@C_yB_x synthesis: formation of LiBC and C-vacancies. LiBC formation is thermodynamically favorable, but we think it can be kinetically avoided due to its fundamental structural difference from xLi@C_yB_x. C-vacancies, established for other Group 14 clathrates, we think are too costly a way to stabilize Li insertion in comparison to B substitution, especially when boron is accessible.

Here is what we have not done, nor do we think we can do:

1. Find the global minimum B substitution pattern for each stuffed clathrate.
2. Search in a random way for alternative structures of each stoichiometry.
3. Come up with a criterion for deciding for any $C_x(LiB)_y$ composition which clathrate structure will be taken up.
4. Calculate the activation energies for isomer interconversion.

Several (many) structures, all stabilized and of similar enthalpy, emerge for Li-doped, B-substituted carbon clathrates. And all these are likely to be kinetically persistent, i.e., to have large barriers to interconvert at P = 1 atm and T = 298 K — they are, after all, strongly bonded organic molecules. We believe the consequence of these two facts points to a variety of possible outcomes when a way is found (it will be!) to synthesize Li-doped, B-substituted clathrates — and that an amorphous material is a likely product. The entropy effect arising from many ways of distributing B substitution sites will also favor the formation of amorphous material.

COMPUTATIONAL METHODS

All solid-state electronic structure calculations are carried out using the Vienna *ab initio* simulation package (VASP-5.3.5),[108−111] with the projector augmented-wave (PAW) potentials[112,113] and PBE functional.[114,115] K points are automatically generated using the Monkhorst−Pack scheme[116] for Clathrates I and VII that have cubic unit cells, and their Li-doped and B-substituted derivatives. For Clathrates II, IV, and H with hexagonal unit cells, the Γ-centered K-mesh is used. The density of K points is systematically increased until the enthalpy converges within 0.0001 eV/atom. A plane-wave energy cutoff of 520 eV is used throughout. COHPs are obtained using the program LOBSTER-1.2.0.[117,118] We employ FINDSYM[119,120] to find the space group symmetry of our optimized structures. The five $8Li@C_{38}B_8$ isomers with the largest possible subgroups of the cubic $Pm\bar{3}m$ space group of Clathrate I (shown in Figure S8) are obtained using ToposPro,[121] which is also used to check all the topologies. All unit cell structures are plotted using VESTA 3.1.6.[122] The neopentane and $B(CH_3)_4^-$ calculations in section S3 in the SI are carried out using the GAMESS-US program package[123,124] with the PBE functional and cc-pVTZ basis set.[125] Their natural bond orbital[126] analyses are done with NBO 6.0.[127] Molecular structures are plotted using MacMolPlt 7.4.4.[128]

Two band gaps are reported for each compound, one from the conventional DFT DOS calculation, the other calculated at the G0W0 level of theory. From the DFT calculated band structure, it is clear between which k points the band gap occurs, and then we calculate G0W0 band gap by subtracting G0W0 energy levels of HOCO and LUCO at the respective k points. While the G0W0 band gaps are more quantitatively meaningful, qualitative discussions such as COHPs are based on the conventional DFT DOS. Despite the substantial difference in quantity (up to 1.7 eV) between the two sets of band gaps, they vary with the same trend, i.e., clathrates with more 90° bond angles have smaller band gaps, and Li doping−B substitution reduces band gaps.

DOI: 10.1021/jacs.5b07883
J. Am. Chem. Soc. 2015, 137, 12639−12652

■ ASSOCIATED CONTENT

Supporting Information

The Supporting Information is available free of charge on the ACS Publications website at DOI: 10.1021/jacs.5b07883.

Figures S1−S25 and Table S1, giving frontier crystal orbital densities of 2Li@C_{12}; COHP analysis of 2Li@$C_{10}B_2$; molecular calculation results and analyses of neopentane and $B(CH_3)_4^-$; substitution schemes for 8Li@$C_{38}B_8$; further discussions of Clathrates IV, H, and II, and their Li insertion and B substitution; further discussion on 8Li@$C_{44}\square_2$ (PDF)

Coordinates of all unit cells (TXT)

■ AUTHOR INFORMATION

Corresponding Author

*rh34@cornell.edu

Notes

The authors declare no competing financial interest.

■ ACKNOWLEDGMENTS

We thank Andreas Hermann, Guoying Gao, Peng Xu, and Martin Rahm for enlightening discussion, and Yuri Grin for bringing some references to our attention. We thank Mark Gordon and Michael Schmidt for their continuing development of the GAMESS-US program suite. We thank Frank Weinhold for providing us with the program NBO 6.0. T.Z. thanks Natural Sciences and Engineering Research Council of Canada for the Banting Postdoctoral Fellowship (201211BAF-303459-236530). R.H. is grateful to the National Science Foundation for its financial support (CHE-1305872). D.M.P. is grateful to the Russian Government (Grant 14.B25.31.0005) for support. T.A.S. acknowledges support from DARPA (Grant W31P4Q-13-1-0005). R.N. thanks Collegium Helveticum, Common Institution of ETH, and the University of Zürich.

■ REFERENCES

(1) Pauling, L.; Marsh, R. E. *Proc. Natl. Acad. Sci. U. S. A.* **1952**, *38*, 112−118.

(2) Mandelcorn, L. *Chem. Rev.* **1959**, *59*, 827−839.

(3) Buffett, B. A. *Annu. Rev. Earth Planet. Sci.* **2000**, *28*, 477−407.

(4) Momma, K. *J. Phys.: Condens. Matter* **2014**, *26*, 103203.

(5) Baitinger, M.; Böhme, B.; Ormeci, A.; Grin, Y. Solid State Chemistry of Clathrate Phases: Crystal Structure, Chemical Bonding and Preparation Routes. In *The Physics and Chemistry of Inorganic Clathrates*; Nolas, G. S., Ed.; Springer Series in Materials Science, Vol. *199*; Springer : Netherlands, 2014; pp 35−64.

(6) Kovnir, K. A.; Shevelkov, A. V. *Russ. Chem. Rev.* **2004**, *73*, 923−938.

(7) Beekman, M.; Nolas, G. S. *J. Mater. Chem.* **2008**, *18*, 842−851.

(8) Christensen, M.; Johnsen, S.; Iversen, B. B. *Dalton Trans.* **2010**, *39*, 978−992.

(9) Chan, K. S.; Miller, M. A.; Liang, W.; Ellis-Terrell, C.; Peng, X. *J. Mater. Sci.* **2014**, *49*, 2723−2733.

(10) Mélinon, P. In *SiC cage like based materials in Silicon Carbide—Materials, Processing and Applications in Electronic Devices*; Mukherjee, M., Ed.; InTech: Croatia, 2011; pp 23−52.

(11) San-Miguel, A.; Toulemonde, P. *High Pressure Res.* **2005**, *25*, 159−185.

(12) Cros, C.; Pouchard, M. *C. R. Chim.* **2009**, *12*, 1014−1056.

(13) http://rcsr.anu.edu.au/

(14) O'Keeffe, M.; Peskov, M. A.; Ramsden, S. J.; Yaghi, O. M. *Acc. Chem. Res.* **2008**, *41*, 1782−1789.

(15) http://www.iza-structure.org/databases/

(16) Sikirić, M. D.; Delgado-Friedrichs, O.; Deza, M. *Acta Crystallogr., Sect. A: Found. Crystallogr.* **2010**, *66*, 602−615.

(17) Delgado-Friedrichs, O.; O'Keeffe, M. *Acta Crystallogr., Sect. A: Found. Crystallogr.* **2010**, *66*, 637−639.

(18) Karttunen, A. J.; Fässler, T. F.; Linnolahti, M.; Pakkanen, T. A. *Inorg. Chem.* **2011**, *50*, 1733−1742.

(19) O'Keeffe, M.; Adams, G. B.; Sankey, O. F. *Philos. Mag. Lett.* **1998**, *78*, 21−28.

(20) Kosyakov, V. I.; Shestakov, V. I. *Chem. Sustain. Devel.* **2000**, *8*, 155−160.

(21) Timoshevskii, V.; Connétable, D.; Blase, X. *Appl. Phys. Lett.* **2002**, *80*, 1385−1387.

(22) Wang, J.-T.; Chen, C.; Wang, D.-S.; Mizuseki, H.; Kawazoe, Y. *J. Appl. Phys.* **2010**, *107*, 063507.

(23) Nesper, R.; Vogel, K.; Blöchl, P. E. *Angew. Chem., Int. Ed. Engl.* **1993**, *32*, 701−703.

(24) Perottoni, C.; da Jornada, J. A. H. *J. Phys.: Condens. Matter* **2001**, *13*, 5981−5998.

(25) Mujica, A.; Pickard, C. J.; Needs, R. J. *Phys. Rev. B: Condens. Matter Mater. Phys.* **2015**, *91*, 214104.

(26) Blank, V. D.; Buga, S. G.; Dubitsky, G. A.; Serebryanaya, N. R.; Popov, M. Yu.; Sundqvist, B. *Carbon* **1998**, *36*, 319−343.

(27) Rey, N.; Muñoz, A.; Rodríguez-Hernández, P.; San Miguel, A. *J. Phys.: Condens. Matter* **2008**, *20*, 215218.

(28) Colonna, F.; Fasolino, A.; Meijer, E. J. *Solid State Commun.* **2012**, *152*, 180−184.

(29) Blase, X.; Bustarret, E.; Chapelier, C.; Klein, T.; Marcenat, C. *Nat. Mater.* **2009**, *8*, 375−382.

(30) Blase, X.; Gillet, P.; San Miguel, A.; Mélinon, P. *Phys. Rev. Lett.* **2004**, *92*, 215505.

(31) Connétable, D. *Phys. Rev. B: Condens. Matter Mater. Phys.* **2010**, *82*, 075209.

(32) Baburin, I. A.; Proserpio, D. M.; Saleev, V. A.; Shipilova, A. V. *Phys. Chem. Chem. Phys.* **2015**, *17*, 1332−1338.

(33) Balaban, A. T.; Rentia, C. C.; Ciupitu, E. *Rev. Roum. Chim.* **1968**, *13*, 231−247.

(34) Adams, G. B.; O'Keeffe, M.; Demkov, A. A.; Sankey, O. F.; Huang, Y.-M. *Phys. Rev. B: Condens. Matter Mater. Phys.* **1994**, *49*, 8048−8053.

(35) Benedek, G.; Galvani, E.; Sanuinetti, S. *Nuovo Cimento Soc. Ital. Fis., D* **1995**, *17*, 97−102.

(36) Benedek, G.; Colombo, L. *Mater. Sci. Forum* **1996**, *232*, 247−274.

(37) Ribeiro, F. J.; Tangney, P.; Louie, S. G.; Cohen, M. L. *Phys. Rev. B: Condens. Matter Mater. Phys.* **2006**, *74*, 172101.

(38) Yamanaka, S. *Dalton Trans.* **2010**, *39*, 1901−1915.

(39) Yamanaka, S.; Kubo, A.; Inumaru, K.; Komaguchi, K.; Kini, N. S.; Inoue, T.; Irifune, T. *Phys. Rev. Lett.* **2006**, *96*, 076602.

(40) Yamanaka, S.; Kini, N. S.; Kubo, A.; Jida, S.; Kuramoto, H. *J. Am. Chem. Soc.* **2008**, *130*, 4303−4309.

(41) Chen, X.; Yamanaka, S.; Sako, K.; Inoue, K. Y.; Yasukawa, M. *Chem. Phys. Lett.* **2002**, *356*, 291−297.

(42) Kasper, J.; Hagenmuller, P.; Pouchard, M.; Cros, C. *Science* **1965**, *150*, 1713−1714.

(43) Cros, C.; Pouchard, M.; Hagenmuller, P. *C. R. Acad. Sci. Paris* **1965**, *260*, 4764−4767.

(44) Gallmeier, J.; Schaefer, H.; Weiss, A. *Z. Naturforsch., B: J. Chem. Sci.* **1967**, *22*, 1080.

(45) Connétable, D.; Timoshevskii, V.; Masenelli, B.; Beille, J.; Marcus, J.; Barbara, B.; Saitta, A. M.; Rignanese, G.-M.; Mélinon, P.; Yamanaka, S.; Blase, X. *Phys. Rev. Lett.* **2003**, *91*, 247001.

(46) Liang, Y.; Böhme, B.; Reibold, M.; Schnelle, W.; Schwarz, U.; Baitinger, M.; Lichte, H.; Grin, Y. *Inorg. Chem.* **2011**, *50*, 4523−4528.

(47) Liang, Y.; Böhme, B.; Ormeci, A.; Borrmann, H.; Pecher, O.; Haarmann, F.; Schnelle, W.; Baitinger, M.; Grin, Y. *Chem. - Eur. J.* **2012**, *18*, 9818−9822.

(48) We should note that, if we were to begin with 8 Li *atoms* in our thermochemical estimate, instead of bulk Li, ΔH would be 0.66 eV/Li, since the experimental cohesive energy of Li is 1.65 eV/Li:

DOI: 10.1021/jacs.5b07883
J. Am. Chem. Soc. 2015, 137, 12639−12652

Gschneidner, K. A. *Solid State Phys.* **1964**, *16*, 275−426. Our DFT calculation overestimates the Li cohesive energy to be 1.90 eV/Li, which is qualitatively acceptable. Strictly speaking, we should add the cohesive enthalpy, instead of the cohesive energy, to obtain the Li-doping enthalpy relative to Li atoms. However, since the *PV* term with P = 1 atm and V = 22.4 L (1 mol of Li atoms) amounts to 0.02 eV, which is insignificant compared to the cohesive energy of Li, we simply add the cohesive energy to the original doping enthalpy relative to Li solid.
(49) Kröner, R.; Peters, K.; von Schnering, H. G.; Nesper, R. *Z. Kristallogr. - New Cryst. Struct.* **1998**, *213*, 667−668.
(50) von Schnering, H. G.; Kröner, R.; Menke, H.; Peters, K.; Nesper, R. *Z. Kristallogr. - New Cryst. Struct.* **1998**, *213*, 677−678.
(51) Jung, W.; Lörincz, J.; Ramlau, R.; Borrmann, H.; Prots, Y.; Haarmann, F.; Schnelle, W.; Burkhardt, U.; Baitinger, M.; Grin, Y. *Angew. Chem., Int. Ed.* **2007**, *46*, 6725−6728.
(52) Roudebush, J. H.; Tsujii, N.; Hurtando, A.; Hope, H.; Grin, Yu.; Kauzlarich, S. M. *Inorg. Chem.* **2012**, *51*, 4161−4169.
(53) Toberer, E. S.; Christensen, M.; Iversen, B. B.; Snyder, G. J. *Phys. Rev. B: Condens. Matter Mater. Phys.* **2008**, *77*, 075203.
(54) Saramat, A.; Svensson, G.; Palmqvist, A. E. C.; Stiewe, C.; Mueller, E.; Platzek, D.; Williams, S. G. K.; Rowe, D. M.; Bryan, J. D.; Stucky, G. D. *J. Appl. Phys.* **2006**, *99*, 023708.
(55) Chakoumakos, B. C.; Sales, B. C.; Mandrus, D. G.; Nolas, G. S. *J. Alloys Compd.* **2000**, *296*, 80−86.
(56) Li, Y.; Garcia, J.; Chen, N.; Liu, L.; Li, F.; Wei, Y.; Bi, S.; Cao, G.; Feng, Z. S. *J. Appl. Phys.* **2013**, *113*, 203908.
(57) Uemura, T.; Akai, K.; Koga, K.; Tanaka, T.; Kurisu, H.; Yamamoto, S.; Kishimoto, K.; Koyanagi, T.; Matsuura, M. *J. Appl. Phys.* **2008**, *104*, 013702.
(58) Some comparative insight might be gained from the B−B, B−C, and C−C distances within one molecule—we have this in *o*-$C_2B_{10}H_{12}$. Though the bonding is rather different from our clathrates (the carborane has delocalized electron-deficient bonding), we see in it 1.67 Å C−C bonds, 1.71−1.72 Å C−B bonds, and 1.77 Å B:B bonds: Lee, S.; Dowben, P. A.; Wen, A. T.; Hitchcock, A. P.; Glass, J. A.; Spencer, J. T. *J. Vac. Sci. Technol., A* **1992**, *10*, 881−885.
(59) Allen, F. H. *Acta Crystallogr., Sect. B: Struct. Sci.* **2002**, *58*, 380−388.
(60) Zhu, D.; Kochi, J. K. *Organometallics* **1999**, *18*, 161−172.
(61) Rhine, W. E.; Stucky, G.; Peterson, S. W. *J. Am. Chem. Soc.* **1975**, *97*, 6401−6406.
(62) Pfeiffer, M.; Stey, T.; Jehle, H.; Klüpfel, B.; Malisch, W.; Chandrasekhar, V.; Stalke, D. *Chem. Commun.* **2001**, 337−338.
(63) Vojteer, N.; Hillebrecht, H. *Angew. Chem., Int. Ed.* **2006**, *45*, 165−168.
(64) Vojteer, N.; Sagawe, V.; Stauffer, J.; Schroeder, M.; Hillebrecht, H. *Chem. - Eur. J.* **2011**, *17*, 3128−3135.
(65) Vojteer, N.; Schroeder, M.; Röhr, C.; Hillebrecht, H. *Chem. - Eur. J.* **2008**, *14*, 7331−7342.
(66) Aoyagi, S.; Nishibori, E.; Sawa, H.; Sugimoto, K.; Takata, M.; Miyata, Y.; Kitaura, R.; Shinohara, H.; Okada, H.; Sakai, T.; Ono, Y.; Kawachi, K.; Yokoo, K.; Ono, S.; Omote, K.; Kasama, Y.; Ishikawa, S.; Komuro, T.; Tobita, H. *Nat. Chem.* **2010**, *2*, 678−683.
(67) Okada, H.; Komuro, T.; Sakai, T.; Matsuo, Y.; Ono, Y.; Omote, K.; Yokoo, K.; Kawachi, K.; Kasama, Y.; Ono, S.; Hatakeyama, R.; Kaneko, T.; Tobita, H. *RSC Adv.* **2012**, *2*, 10624−10631.
(68) There is no small size limit on clathrates, of course. One can even think about inserting atoms into diamond lattices, and we will have occasion below to mention this.
(69) Hedin, L. *Phys. Rev.* **1965**, *139*, A796−A823.
(70) Onida, G.; Reining, L.; Rubio, A. *Rev. Mod. Phys.* **2002**, *74*, 601−659.
(71) Shishkin, M.; Kresse, G. *Phys. Rev. B: Condens. Matter Mater. Phys.* **2006**, *74*, 035101.
(72) Alvarez, S. *Dalton Trans.* **2013**, *42*, 8617−8636.
(73) Shannon, R. D. *Acta Crystallogr., Sect. A: Cryst. Phys., Diffr., Theor. Gen. Crystallogr.* **1976**, *32*, 155−169.
(74) Bondi, A. *J. Phys. Chem.* **1964**, *68*, 441−451.
(75) Batsanov, S. S. *Inorg. Mater.* **2001**, *37*, 871−885.
(76) Dronskowski, R.; Blöchl, P. E. *J. Phys. Chem.* **1993**, *97*, 8617−8624.
(77) The N point is chosen because the HOCO is under the Fermi level at this point (see Figure 2), i.e., for sure it is occupied.
(78) Sevov, S. C. In *Zintl Phases in Intermetallic Compounds, Principles and Practice: Progress*; Westbrook, J. H., Freisher, R. L., Eds.; John Wiley & Sons. Ltd.: Chichester, England, 2002; pp 113−132.
(79) Nesper, R. *Z. Anorg. Allg. Chem.* **2014**, *640*, 2639−2648.
(80) Blake, N. P.; Latturner, S.; Bryan, J. D.; Stucky, G. D.; Metiu, H. *J. Chem. Phys.* **2001**, *115*, 8060−8073.
(81) Blake, N. P.; Bryan, D.; Latturner, S.; Mollnitz, L.; Stucky, G. D.; Metiu, H. *J. Chem. Phys.* **2001**, *114*, 10063−10074.
(82) Zeilinger, M.; van Wüllen, L.; Benson, D.; Kranak, V. F.; Konar, S.; Fässler, T. F.; Häussermann, U. *Angew. Chem., Int. Ed.* **2013**, *52*, 5978−5982.
(83) Standard Thermodynamic Properties of Chemical Substances. In *CRC Handbook of Chemistry and Physics*, 96th ed. (Internet Version); Haynes, W. M., Ed.; CRC Press/Taylor and Francis, Boca Raton, FL, 2016.
(84) Kurakevych, O. O.; Strobel, T. A.; Kim, D. Y.; Muramatsu, T.; Struzhkin, V. V. *Cryst. Growth Des.* **2013**, *13*, 303−307.
(85) Kim, D. Y.; Stefanoski, S.; Kurakevych, O. O.; Strobel, T. A. *Nat. Mater.* **2015**, *14*, 169−173.
(86) Hanfland, M.; Syassen, K.; Christensen, N. E.; Novikov, D. L. *Nature* **2000**, *408*, 174−178.
(87) Oganov, A. R.; Chen, J.; Gatti, C.; Ma, Y.-M.; Yu, T.; Liu, Z.; Glass, C. W.; Ma, Y.-Z.; Kurakevych, O. O.; Solozhenko, V. L. *Nature* **2009**, *457*, 863−867.
(88) Gallmeier, J.; Schäfer, H.; Weiss, A. *Z. Naturforsch., B: J. Chem. Sci.* **1969**, *24*, 665−671.
(89) Mudryk, Y.; Rogl, P.; Paul, C.; Berger, S.; Bauer, E.; Hilscher, G.; Godart, C.; Noël, H. *J. Phys.: Condens. Matter* **2002**, *14*, 7991−8004.
(90) Blase, X. *Phys. Rev. B: Condens. Matter Mater. Phys.* **2003**, *67*, 035211.
(91) Connétable, D.; Blase, X. *Appl. Surf. Sci.* **2004**, *226*, 289−297.
(92) Grochala, W.; Hoffmann, R. *J. Phys. Chem. A* **2000**, *104*, 9740−9749.
(93) Benedek, G.; Galvani, E.; Sanguinetti, S.; Serra, S. *Chem. Phys. Lett.* **1995**, *244*, 339−344.
(94) Bernasconi, M.; Gaito, S.; Benedek, G. *Phys. Rev. B: Condens. Matter Mater. Phys.* **2000**, *61*, 12689−12692.
(95) Schreiner, P. R.; Chernish, L. V.; Gunchenko, P. A.; Tikhonchuk, E.; Yu; Hausmann, H.; Serafin, M.; Schlecht, S.; Dahl, J. E. P.; Carlson, R. M. K.; Fokin, A. A. *Nature* **2011**, *477*, 308−311.
(96) Momma, K. *J. Phys.: Condens. Matter* **2014**, *26*, 103203.
(97) Bobev, S.; Sevov, S. C. *Mater. Res. Soc. Symp. Proc.* **2000**, *626*, Z13.5.
(98) We define the radius as the average distance from the center of the adamantane cage in diamond to the 10 vertices of the cage. There are four distances of 1.54 Å and six of 1.78 Å.
(99) Wörle, M.; Nesper, R. *Angew. Chem., Int. Ed.* **2000**, *39*, 2349−2353.
(100) Liu, Z.; Qu, X.; Huang, B.; Li, Z. *J. Alloys Compd.* **2000**, *311*, 256−264.
(101) Hermann, A.; McSorley, A.; Ashcroft, N. W.; Hoffmann, R. *J. Am. Chem. Soc.* **2012**, *134*, 18606−18618.
(102) Wörle, M.; Nesper, R.; Mair, G.; Schwarz, M.; von Schnering, H. G. *Z. Anorg. Allg. Chem.* **1995**, *621*, 1153−1159.
(103) Dubois, F.; Fässler, T. F. *J. Am. Chem. Soc.* **2005**, *127*, 3264−3265.
(104) Kaltzoglou, A.; Hoffmann, S. D.; Fässler, T. F. *Eur. J. Inorg. Chem.* **2007**, *2007*, 4162−4167.
(105) Beekman, M.; Nolas, G. S. *Int. J. Appl. Ceram. Technol.* **2007**, *4*, 332−338.
(106) Zhao, J.-T.; Corbett, J. D. *Inorg. Chem.* **1994**, *33*, 5721−5726.
(107) The *Cc* 8Li@$C_{44}\square_2$ on the right-hand side of the reaction has the vacancies on two far apart 24*k* sites. It is lower in enthalpy by 0.24

DOI: 10.1021/jacs.5b07883
J. Am. Chem. Soc. 2015, 137, 12639−12652

eV/Li than the structure with the vacancies on two non-coplanar 6*c* sites. The reason why vacancies tend to occupy 24*k*, instead of the more conventional 6*c* sites, is left for future study. This order of enthalpy difference does not affect the endothermicity of the reaction, and thus our basic conclusion is not affected by which $8Li@C_{44}\square_2$ structure is used.

(108) Kresse, G.; Hafner, J. *Phys. Rev. B: Condens. Matter Mater. Phys.* **1993**, *47*, 558−561.
(109) Kresse, G.; Hafner, J. *Phys. Rev. B: Condens. Matter Mater. Phys.* **1994**, *49*, 14251−14269.
(110) Kresse, G.; Furthmüller, J. *Comput. Mater. Sci.* **1996**, *6*, 15−50.
(111) Kresse, G.; Furthmüller, J. *Phys. Rev. B: Condens. Matter Mater. Phys.* **1996**, *54*, 11169−11186.
(112) Blöchl, P. E. *Phys. Rev. B: Condens. Matter Mater. Phys.* **1994**, *50*, 17953−17979.
(113) Kresse, G.; Joubert, D. *Phys. Rev. B: Condens. Matter Mater. Phys.* **1999**, *59*, 1758−1775.
(114) Perdew, J. P.; Burke, K.; Ernzerhof, M. *Phys. Rev. Lett.* **1996**, *77*, 3865−3868.
(115) Perdew, J. P.; Burke, K.; Ernzerhof, M. *Phys. Rev. Lett.* **1997**, *78*, 1396.
(116) Monkhorst, H. J.; Pack, J. D. *Phys. Rev. B* **1976**, *13*, 5188−5192.
(117) Deringer, V. L.; Tchougréeff, A. L.; Dronskowski, R. *J. Phys. Chem. A* **2011**, *115*, 5461−5466.
(118) Maintz, S.; Deringer, V. L.; Tchougréeff, A. L.; Dronskowski, R. *J. Comput. Chem.* **2013**, *34*, 2557−2567.
(119) *ISOTROPY Software Suite*, iso.byu.edu.
(120) Stokes, H. T.; Hatch, D. M. *J. Appl. Crystallogr.* **2005**, *38*, 237−238.
(121) Blatov, V. A.; Shevchenko, A. P.; Proserpio, D. M. *Cryst. Growth Des.* **2014**, *14*, 3576−3586.
(122) Momma, K.; Izumi, F. *J. Appl. Crystallogr.* **2011**, *44*, 1272−1276.
(123) Schmidt, M. W.; Baldridge, K. K.; Boatz, J. A.; Elbert, S. T.; Gordon, M. S.; Jensen, J. H.; Koseki, S.; Matsunaga, N.; Nguyen, K. A.; Su, S.; Windus, T. L.; Dupuis, S.; Montgomery, J. A. *J. Comput. Chem.* **1993**, *14*, 1347−1363.
(124) Gordon, M. S.; Schmidt, M. W. Advances in electronic structure theory: GAMESS a decade later. In *Theory and Applications of Computational Chemistry: The First Forty Years*; Dykstra, C. E., Frenking, G., Kim, K. S., Scuseria, G. E., Eds.; Elsevier: Amsterdam, 2005; pp 1167−1189.
(125) Dunning, T. H. *J. Chem. Phys.* **1989**, *90*, 1007−1023.
(126) Foster, J. P.; Weinhold, F. *J. Am. Chem. Soc.* **1980**, *102*, 7211−7218.
(127) Glendening, E. D.; Landis, C. R.; Weinhold, F. *J. Comput. Chem.* **2013**, *34*, 1429−1437.
(128) Bode, B. M.; Gordon, M. S. *J. Mol. Graphics Modell.* **1998**, *16*, 133−138.

DOI: 10.1021/jacs.5b07883
J. Am. Chem. Soc. 2015, 137, 12639−12652